

RESEARCH MEMORANDUM

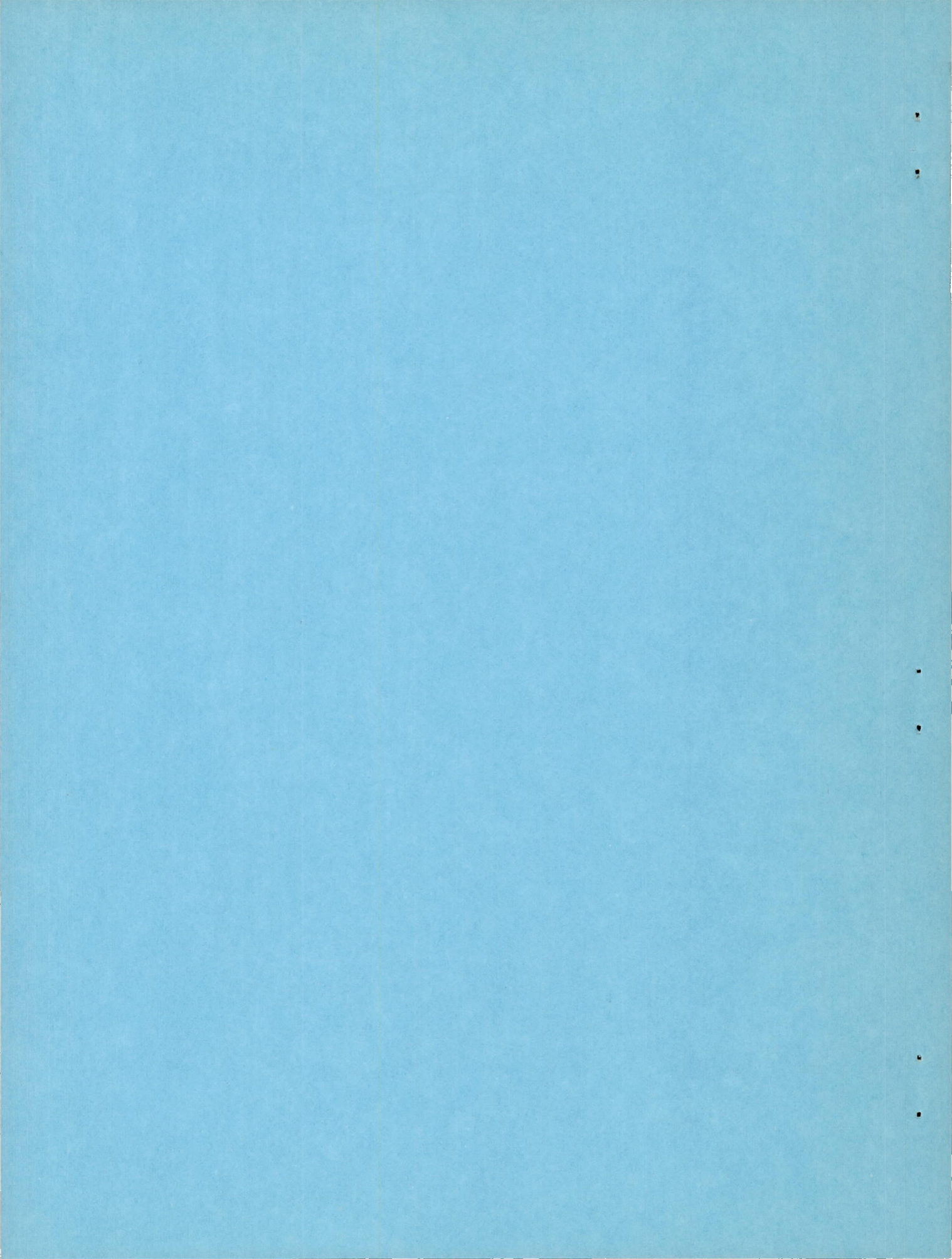
EFFECT OF MACH NUMBER ON PERFORMANCE OF AN
AXIAL-FLOW COMPRESSOR ROTOR-BLADE ROW

By Paul D. Dugan, John J. Mahoney
and William A. Benser

Flight Propulsion Research Laboratory
Cleveland, Ohio

NATIONAL ADVISORY COMMITTEE
FOR AERONAUTICS

WASHINGTON
September 28, 1948



NATIONAL ADVISORY COMMITTEE FOR AERONAUTICS

RESEARCH MEMORANDUMEFFECT OF MACH NUMBER ON PERFORMANCE OF AN
AXIAL-FLOW-COMPRESSOR ROTOR-BLADE ROWBy Paul D. Dugan, John J. Mahoney
and William A. Benser

SUMMARY

An investigation was conducted to study the influence of high relative inlet Mach number on the performance of a highly loaded blade row. Twenty-nine NACA 65-series rotor blades, designed for axial inlet velocity, were installed in a compressor rotor with a tip diameter of 14 inches and a hub-to-tip diameter ratio of approximately 0.8. Static and total pressure, total temperature, and flow-angle surveys were taken upstream and downstream of the rotor row to study the blade-row performance and total-pressure ratio and efficiency. A range of weight flow was investigated for equivalent tip speeds ranging from 300 to 915 feet per second, corresponding to a range of relative inlet Mach number of 0.30 to 0.90 at the mean radius.

Above a relative inlet Mach number of 0.70, the results at the mean-radius blade section at the design angle of attack, indicated good correlation between the turning angle of 19° for this investigation and low-speed cascade results. At lower relative inlet Mach numbers, the turning angles for this investigation were approximately 1° lower than the value of 19° predicted by low-speed cascade runs. Turning angles increased about 1° as the relative inlet Mach number increased from 0.30 to 0.90 in accordance with high-speed two-dimensional cascade data. Three-dimensional effects prevented the occurrence of a force-break decrease in turning angle predicted by two-dimensional results. The efficiency gradually decreased from 0.950 to 0.915 as the relative inlet Mach number increased from 0.30 to 0.82, but at Mach numbers above 0.82 the efficiency rapidly decreased. Therefore, the ideal operating condition for this blade design gave a total-pressure ratio of 1.35, an adiabatic efficiency of 0.915, and a relative inlet Mach number of 0.82.

The calculated performance values for a theoretical complete stage, based on a symmetrical velocity diagram at the mean radius, indicated a total-pressure ratio of 1.44 with an adiabatic

efficiency of 0.886 at a relative inlet Mach number of 0.80. A peak total-pressure ratio of 1.48 at a relative inlet Mach number of 0.86 was indicated.

INTRODUCTION

A high pressure ratio per stage is necessary to develop compact axial-flow compressors for aircraft application. An analysis of the effect of basic design variables on the performance of axial-flow compressors (reference 1) indicates that the relative inlet Mach number of the air with respect to the blades is an important factor in determining the optimum pressure ratio. High-stage pressure ratios, achieved by increasing the relative inlet Mach number beyond the present limiting value (approximately 0.70), can be realized only if the loss in efficiency due to increased relative inlet Mach number is not excessive. Two-dimensional high-speed cascade results (reference 2) lead to the prediction that the combination of high blade loading and high relative inlet Mach number may produce a stage pressure ratio of the order of 1.4.

In order to study the possibility of utilizing the high blade loading and high relative inlet Mach number in axial-flow compressors and to study the applicability of two-dimensional cascade data to high-speed rotating compressors, a rotor blade row was designed and constructed at the NACA Langley Field laboratory and investigated at the NACA Cleveland laboratory. The blade row was designed on the basis of results of a stationary cascade investigation of NACA 65-series airfoils (references 2 to 4), had a tip diameter of 14 inches with a hub-to-tip diameter ratio of 0.8 at the entrance to the blades, and contained 29 blades with a constant solidity of 1.2.

In this investigation, the relative inlet Mach number at the mean radius of the blade was varied from 0.30 to 0.90 over a range of weight flows at rotor-tip speeds varying from 300 to 915 feet per second. From the results of these runs, the effects of relative inlet Mach number on the blade-row performance were obtained and the limiting practical value of relative inlet Mach number for this blade design was determined. The rotor performance is compared with the performance predicted by two-dimensional cascade data. The total-pressure ratios and efficiencies, determined from the rotor runs, were used to predict the performance of a theoretical axial-flow stage based on a symmetrical velocity diagram.

SYMBOLS

The following symbols are used herein:

c_p	specific heat at constant pressure, Btu/(lb)(°F)
g	standard acceleration due to gravity, 32.174 (ft)/(sec)(sec)
J	mechanical equivalent of heat, 778.26 (ft-lb/Btu)
M'	relative inlet Mach number, ratio of relative inlet velocity to local velocity of sound
N	rotor speed, (rpm)
P	absolute total pressure, (lb/sq ft)
r	radius to blade element, (ft)
T	total temperature, (°R)
U	velocity of blade at any radius r , (ft/sec)
V	absolute air velocity, (ft/sec)
V'	air velocity relative to rotor, (ft/sec)
W	weight flow, (lb/sec)
$\frac{W\sqrt{\theta}}{\delta}$	equivalent weight flow corrected to NACA standard sea-level conditions, (lb/sec)
α	angle of attack, angle between blade chord and entering air velocity relative to rotor, (deg)
β	stagger angle, angle between compressor axis and air velocity relative to rotor, (deg)
γ	ratio of specific heats, (c_p/c_v) 1.3947 for normal air
η_{ad}	adiabatic efficiency
θ	turning angle, angle between entering and leaving relative air velocities, (deg)
ρ	density, (lb/cu ft)

Subscripts:

- e equivalent velocity vectors based on constant axial velocity diagram
- h hub
- t blade tip
- z axial
- θ tangential
- 1 inlet measuring station
- 2 outlet measuring station

APPARATUS

Compressor Blading

The rotor blades for this investigation were designed at the NACA Langley Field laboratory on the basis of two-dimensional cascade data. The following design assumptions were made:

1. NACA 65-series rotor blades with blade camber and angle of attack for optimum pressure distribution
2. Constant axial component and no whirl component of velocity at inlet
3. No change in axial velocity across blade row
4. Approximately constant energy addition from hub to tip
5. Relative inlet Mach number of 0.72 with inlet stagger angle of 57.4° and turning angle of 19° at blade mean radius
6. 29 blades with constant solidity of 1.2
7. Constant tip diameter of 14 inches and hub-to-tip diameter ratio of 0.8 at inlet to blades

These blades were installed in the rotor of a variable-component compressor, which had a constant tip diameter of 14 inches and a hub diameter that tapered from 11.17 inches at the inlet survey station

to 11.55 inches at the outlet survey station. This hub taper was slightly greater than that required to maintain constant axial velocity across the blade row at design operating conditions. The clearance between the blade tip and the casing was 0.020 inch.

Design values for the root, mean, and tip blade sections are shown in the following table:

	Blade section		
	65-(14)10	65-(9.6)09	65-(7.3)08
	Root radius	Mean radius	Tip radius
Stagger angle, (deg)	54.3	57.4	60.0
Turning angle, (deg)	24.6	19.0	15.6
Angle of attack, (deg)	17.6	13.0	10.0
Relative inlet Mach number	.66	.72	.77
Chord, (in.)	1.460	1.641	1.822
Solidity	1.2	1.2	1.2

Compressor Installation

The compressor installation is schematically shown in figure 1. In this installation, air was drawn in from the test cell through a 14-inch thin-plate orifice, which was mounted on the end of an orifice tank, and flowed through a motor-operated inlet valve of the butterfly type into a depression tank (4 ft in diameter by 6 ft in length). The inlet valve controlled the total pressure at the compressor inlet. A series of screens and a 3-by-3-inch-vaned honeycomb in the depression tank insured smooth uniform flow through a bellmouthed inlet into the compressor. The air discharged from a collector through two pipes into the laboratory exhaust system. Air flow was controlled by a motor-driven butterfly valve in the outlet ducting.

Two 225-horsepower dynamometers, coupled in tandem, were used to drive the rotor through a speed increaser with a ratio of 7.25:1.

INSTRUMENTATION

Air flow through the compressor was calculated from the pressure drop across a standard thin-plate orifice, mounted on the end of an orifice tank, and the test-cell temperature, which was measured by four iron-constantan thermocouples.

Temperature measurements were taken in the depression tank by four probes, each containing four iron-constantan thermocouples. These probes were equally spaced around the circumference of the depression tank and were $1/3$ diameter from the tank wall. The velocity in this tank was sufficiently small that the temperatures measured at this station could be considered stagnation values. Because only ambient-air runs were made, the heat transfer was negligible and no lagging was used. The observed temperature in the depression tank was considered as the inlet total temperature.

Pressure and yaw survey station 1 was located 0.38 inch upstream of the leading edge of the blade tip, and pressure and yaw survey station 2 was located 0.58 inch downstream of the trailing edge of the blade tip. A single total-pressure survey probe (fig. 2) was installed at each station for the purpose of measuring total pressure upstream and downstream of the rotor. Flow-angle measurements at each station were obtained from a single radial survey with a claw-type yaw tube of the type shown in figure 2. The static-pressure survey probes used at stations 1 and 2 are also shown in figure 2. Both static-pressure probes were oriented in the direction of the flow by balancing the pressures obtained from separate static-pressure taps on each side of the instrument. All pressures were measured in inches of tetrabromoethane as differentials from the depression-tank pressure. Readings of total pressure, static pressure, and absolute air angles were taken at four radial positions at both stations 1 and 2. These radial positions were selected as the centers of four equal radial increments across the annulus.

Outlet-total-temperature measurements were obtained at the centers of four equal radial increments by means of four thermocouple rakes, each having four probes, as illustrated in figure 2. The rakes were located 3 inches downstream of the rotor-blade trailing edge and were lined up with the direction of air flow within the permissible yaw angle as determined by calibration.

Compressor speed was controlled electronically within ± 10 rpm and was frequently checked with a chronometric tachometer.

Accuracy of Measurement

The estimated accuracy of the method of measurement used in this investigation is as follows:

Pressure, percentage of dynamic head	±1.0
Absolute air angles, degrees	±0.3
Inlet temperature, °F	±0.5
Outlet temperature, °F	±1.0
Compressor speed, rpm	±10.0

Outlet total temperatures were insufficiently accurate to permit the determination of efficiencies by temperature rise but they were satisfactory for determining densities and velocities at the outlet of the blade row. Comparison of the integrated weight flows upstream and downstream of the rotor with the orifice-measured weight flow provided a check on the accuracy of instrumentation. In general, these integrated values of weight flow upstream and downstream of the rotor checked the orifice-measured values within ±3.0 percent over the entire range of weight flow for each tip speed except at extremely high or low flows.

PROCEDURE

For this investigation, the equivalent tip speed of the blade row was varied from 300 to 915 feet per second. The pressure in the inlet tank was maintained at 25 inches of mercury absolute at all air flows for the range of tip speeds from 300 to 736 feet per second. Because of the large pressure drop through the inlet ducting at tip speeds above 736 feet per second, the inlet pressure at the higher speeds could not be maintained at 25 inches of mercury absolute. The tip speeds of 765 to 874 feet per second were therefore run at an inlet pressure of 24.0 inches of mercury absolute and the 915 feet per second run was conducted at 23.5 inches of mercury absolute. The range of Reynolds number, based on blade chord, for the run of 765 to 915 feet per second was 437,000 to 648,000, which is well above the critical value of 100,000 to 200,000. The effect of the change in inlet pressure at the higher speeds was therefore considered to be negligible.

At each tip speed investigated, the inlet pressure was held constant and the weight flow was varied by controlling the outlet pressure. For tip speeds from 300 to 835 feet per second, the flow was varied from an approximate maximum to blade stall, as indicated by a negative slope of the pressure-ratio curve. Four flow points in the range of design angle of attack were run at tip speeds of 874 and 915 feet per second.

Calculating Procedure

The over-all total-pressure ratio used in this investigation is the pressure ratio that would be obtained with an isentropic power input to the measured total air flow equal to the actual isentropic power input integrated over the flow passage. This total-pressure ratio is calculated by means of a mechanical integration of the following equation:

$$\frac{P_2}{P_1} = \left\{ \frac{\int_{r_{h,2}}^{r_{t,2}} \left[\left(\frac{P_2}{P_1} \right)^{\frac{\gamma-1}{\gamma}} - 1 \right] \rho_2 V_{z,2} r_2 dr}{\int_{r_{h,2}}^{r_{t,2}} \rho_2 V_{z,2} r_2 dr} + 1 \right\}^{\frac{\gamma}{\gamma-1}} \quad (1)$$

The adiabatic efficiencies referred to herein were obtained by dividing the integrated power due to isentropic pressure rise by the integrated power due to turning, as shown in the following equation:

$$\eta_{ad} = \frac{gJc_p T_1 \int_{r_{h,2}}^{r_{t,2}} \rho_2 V_{z,2} r_2 \left[\left(\frac{P_2}{P_1} \right)^{\frac{\gamma-1}{\gamma}} - 1 \right] dr}{\frac{2\pi N}{60} \left(\int_{r_{h,2}}^{r_{t,2}} \rho_2 V_{z,2} r_2^2 V_{\theta,2} dr - \int_{r_{h,1}}^{r_{t,1}} \rho_1 V_{z,1} r_1^2 V_{\theta,1} dr \right)} \quad (2)$$

The efficiency thus calculated was considered to be more accurate than the adiabatic temperature-rise efficiency because in a single-stage axial-flow compressor the temperature rise is extremely small and a slight error in temperature measurement introduces an appreciable error in efficiency.

RESULTS AND DISCUSSION

Blade-Section Performance

Inasmuch as the hub taper of the blade row was slightly greater than that required for constant axial velocity, the axial velocity increased across the rotor for most operating conditions. In order to permit a comparison with two-dimensional cascade data, all turning angles and angles of attack were corrected to an equivalent diagram having constant axial velocity. This equivalent diagram was based on the recommendation of reference 3 and utilized measured components of whirl velocity and the average of the inlet and outlet axial velocity. The effects of boundary-layer build-up on the outer casing and the rotor-blade-tip clearance caused large gradients of velocity and flow angle in the region of the blade tip and excluded the possibility of accurately evaluating blade-row performance at this point. Similarly, the boundary layer and the hub taper eliminated the possibility of accurately determining blade-row performance for the hub section. All individual blade-row performance evaluations are therefore drawn on the basis of data interpolated for the mean radius position.

Variation of turning angle with angle of attack. - Varying the weight flow W at a constant rotor speed N in axial-flow-compressor investigations results in a variation of the angle of attack α as well as the relative inlet Mach number M' of the air with respect to the blades. Changes in angle of attack are accompanied by equivalent changes in stagger angle β . In figure 3, the turning angle θ with respect to the blades is plotted against angle of attack for the mean-radius blade section at the design tip speed of 736 feet per second. For comparison, the curve of turning angle against angle of attack obtained by interpolation of two-dimensional cascade data (references 3, 4, and unpublished data) for a solidity of 1.2, a camber of 9.6, and stagger angles determined by the blade setting and angle of attack is shown on the same figure. Excellent agreement between the equivalent rotor data and cascade data exists in the region of design angle of attack, which is 13° for this blade section. Considerable deviation exists at both extremities of the range of angle of attack. This deviation may be attributed to a combination of two factors: (1) inadequacy of the use of the equivalent diagram to correct for increases in axial velocity at the extremes of the flow ranges where the axial velocity changes were greatest; and (2) radial-flow effects that were not considered in this investigation. True or measured turning angles are also shown on figure 3. This entire curve is more nearly parallel to that predicted by two-dimensional cascade data than is the equivalent turning-angle curve. In comparison with the equivalent turning-angle

curve, the true turning-angle curve is displaced to the right because the angle of attack changes as the axial-velocity variation is taken into account. The turning angle for design angle of attack of 13° is, however, 1.5° higher than the predicted angle of 19° . The relative inlet Mach number for the compressor-blade data was approximately 0.70 as compared with a value of 0.10 for the two-dimensional cascade data.

Effect of relative inlet Mach number on turning angle. - In figure 4, the equivalent turning angles θ_e and the relative inlet Mach numbers M' for all equivalent tip speeds $U_t/\sqrt{\theta}$ investigated are plotted against equivalent angle of attack α_e . A cross plot of equivalent turning angle for design angle of attack against relative inlet Mach number (fig. 5) indicates a 1° increase in equivalent turning angle as the relative inlet Mach number is increased from 0.30 to 0.90. This increase in equivalent turning angle was also observed in the high-speed two-dimensional cascade data (reference 2). The equivalent turning angle obtained at low relative inlet Mach numbers are approximately 1° below the value of 19° predicted by low-speed cascade results (references 3 and 4). At relative inlet Mach numbers of 0.70 and above, however, the equivalent turning angle of 19° predicted by low-speed cascade results was obtained. Two-dimensional cascade data also show that at a constant angle of attack a force break, or sharp decrease in turning angle, occurs as the relative inlet Mach number exceeds a certain value. The value of this force-break Mach number for design angle of attack interpolated for a solidity of 1.2 is given on figure 5 by the dashed curve. The drop in equivalent turning angle that would be expected above a relative inlet Mach number of 0.81 was not obtained in the rotor investigations. This deviation from predictions may be attributed to three-dimensional effects. Design values of relative inlet Mach number give a tip value that is 0.05 greater than at the mean radius. Because of slight deviations from design inlet conditions and because of boundary-layer effects, however, the extrapolated tip relative inlet Mach number is only 0.015 greater than the mean radius value for the flow giving design angle of attack at the mean radius. Inasmuch as the tip Mach number is greater under actual operating conditions and adverse flow conditions exist at the region of the tip, force break will probably occur first at the blade tip, even though the tip critical Mach number will be slightly higher than the other blade-section critical Mach numbers because of the decrease in blade camber with increasing radius. The occurrence of force break at the blade tip would impose a flow restriction in this region and cause a radial flow towards the compressor hub. Axial-velocity distributions at the rotor inlet and outlet for weight flows

approximating design conditions at the mean radius and tip speeds from 736 to 915 feet per second (fig. 6) show that no appreciable change exists with increasing speed in the inlet velocity distribution, which decreases from hub to tip because of hub curvature. The outlet-axial-velocity distribution maintains a similar profile through the equivalent tip-speed range of 736 feet per second to 835 feet per second. Above this tip speed, there is a decrease in axial velocity at the tip and a corresponding increase in axial velocity over the remainder of the annulus. This shift in velocity distribution verifies the existence of an inward radial flow at a tip speed of 915 feet per second. From the principle of conservation of moment of momentum, any inward radial flow will be accompanied by an increase in whirl velocity along a streamline. In addition, this inward flow would cause an increase in axial velocity at the inner radii, which would relieve the adverse pressure gradients near the trailing edge on the upper surface of the blade, and thus reduce the boundary layer and tendencies for separation near the trailing edge of the blade. The combination of these effects probably maintains the turning angle at the mean radius even though the normal relative inlet Mach number for force break has been exceeded.

Over-all Rotor Performance

Total-pressure ratio. - Total-pressure ratios P_2/P_1 , determined by equation (1), are plotted against corrected weight flow $W\sqrt{\theta}/\delta$ in figure 7. The dashed curve indicates the condition of design angle of attack, based on the equivalent velocity diagram, for the mean radius of the rotor blades. At the lower tip speeds from 300 feet per second to 600 feet per second, the total-pressure-ratio curves have a fairly smooth trend over the entire weight-flow range, and design flow conditions occur near the maximum total-pressure-ratio points on the curves. Higher-speed curves indicate that the design flow conditions occur at the approximate center of the effective weight-flow range. In the low flow region of these total-pressure-ratio curves, a sudden drop in total-pressure ratio with a subsequent constant total-pressure-ratio trend indicates blade stall, and at the high flow end of these curves a rapid decrease in total-pressure ratio indicates the maximum flow limit. At the equivalent tip speed of 915 feet per second, the flow breakdown at the blade tip causes a large increase in axial velocity at the mean radius, and the application of the equivalent velocity diagram results in a reduced weight flow for design angle of attack at the mean radius.

Adiabatic efficiency. - Adiabatic efficiencies for all equivalent tip speeds are plotted against corrected weight flows in figure 8. The design flow condition at the mean radius is indicated by a bar on each of the efficiency curves. This design flow condition is considerably below the peak efficiency of the low-speed curves, but as the speed increases the design flow condition approaches the peak efficiency point of the curves. Efficiency curves for all of the equivalent tip speeds except 300 feet per second are characterized by a nearly constant efficiency over an appreciable range of weight flows. At design speed, this weight-flow range corresponds to a variation in angle of attack at the mean radius from 3° above to 4° below the design value.

Effect of relative inlet Mach number on over-all performance. - In figure 9, the variation in total-pressure ratio and adiabatic efficiency for design geometry of flow at the mean radius are plotted against the relative inlet Mach number. The inflection in the total-pressure-ratio curve at a relative inlet Mach number of approximately 0.82 may be partly caused by the large decrease in adiabatic efficiency at a high relative inlet Mach number and partly caused by a flow breakdown at the blade tip (fig. 6). The adiabatic efficiency gradually decreased from 0.950 to 0.915 as the relative inlet Mach number increased from 0.30 to 0.82. The limiting relative inlet Mach number for this design appears to be 0.82 for at relative inlet Mach numbers above this value the efficiency decreased very rapidly. At a relative inlet Mach number of 0.82, the total-pressure ratio was 1.35 and the adiabatic efficiency was 0.915.

Theoretical Complete-Stage Performance

As shown in reference 1, a symmetrical velocity diagram for an axial-flow stage results in the maximum work input for a given Mach number and blade-loading limitation. If the velocity diagram for the mean radius of this rotor (fig. 10(a)) is converted to a symmetrical diagram for the complete stage (fig. 10(b)) having the same velocities and angles with respect to the rotor, a higher rotor speed and correspondingly greater total-pressure ratio can be obtained. The performance of a full stage based on the symmetrical diagram was therefore calculated by means of the method outlined in reference 1 and by the assumption that the polytropic exponent of compression was the same for the stator-blade row as for the rotor-blade row. Tip losses and effects of variation of conditions with radius were partly accounted for by using the over-all efficiency determined in the rotor investigation to obtain the variation of the static compression exponent with inlet Mach number. No account was taken of the total-pressure loss incurred in imparting

the initial rotation to the air for the symmetrical diagram case. The calculated stage performance values are approximate but they serve to indicate the anticipated stage performance over a range of inlet Mach numbers if the variation of conditions from hub to tip is of the same order of magnitude as for the rotor design reported.

Calculated values of total-pressure ratio and adiabatic efficiency for the complete stage are plotted against relative inlet Mach number in figure 11. For comparison, the isentropic total-pressure-ratio variation with relative inlet Mach number is also shown. A maximum total-pressure ratio of 1.48 is indicated for a relative inlet Mach number of 0.86; at higher Mach numbers the losses are sufficiently severe to offset the increased energy input, and a decrease in total-pressure ratio is indicated. The practical limitation of relative inlet Mach number with regard to efficiency and total-pressure ratio appears to be approximately 0.80 for the complete stage. This relative inlet Mach number gives a total-pressure ratio of 1.44 and an adiabatic efficiency of 0.886.

This efficiency, which is conservative, seems low compared with current single-stage compressors. A direct comparison, however, should not be made between this predicted stage performance and that of existing axial-flow compressor stages. A more correct comparison would be between the predicted performance and a two- or three-stage compressor of conventional design. Because annulus losses, tip-clearance losses, and re-entrance losses in multistage compressors are appreciable, the efficiency of 0.886 indicated for a total-pressure ratio of 1.44 would compare favorably with that expected from a multistage axial-flow compressor of conventional design for comparable total-pressure ratio.

SUMMARY OF RESULTS

From the investigation of the influence of high relative Mach number on the performance of a highly loaded blade row reported herein, the following results were obtained:

1. In the region of design angle of attack at the mean radius, the turning angle of 19° predicted by low-speed cascade results was obtained at relative inlet Mach numbers above 0.70. Below a relative inlet Mach number of 0.70, equivalent turning angles for this investigation were approximately 1° lower than the predicted value of 19° . An increase in equivalent turning angle of approximately 1° occurred as the relative inlet Mach number was increased from 0.30 to 0.90 at design angle of attack, in accordance with the high-speed two-dimensional cascade results. Three-dimensional effects precluded

the occurrence of the force break indicated by two-dimensional investigations.

2. The optimum performance of this blade design was a total-pressure ratio of 1.35 and an adiabatic efficiency of 0.915 for a relative inlet Mach number of 0.82 at the mean radius of the blade. A maximum efficiency of 0.950 for the design angle of attack was obtained at a relative inlet Mach number of 0.30; above a relative inlet Mach number of 0.82 the efficiency rapidly decreased.

3. Calculated performance values for a theoretical full stage based on a symmetrical velocity diagram indicated a total-pressure ratio of 1.44 and an adiabatic efficiency of 0.886 at a relative inlet Mach number of 0.80. The peak total-pressure ratio indicated was 1.48 at a relative inlet Mach number of 0.86.

Flight Propulsion Research Laboratory,
National Advisory Committee for Aeronautics,
Cleveland, Ohio.

REFERENCES

1. Sinnette, John T., Jr.: Some Methods of Analyzing the Effect of Basic Design Variables on Axial-Flow-Compressor Performance. NACA RM No. E7D28, 1947.
2. Bogdonoff, Seymour M.: Performance of Compressor Blade Cascades at High Mach Numbers. NACA RM No. L7D11a, 1947.
3. Bogdonoff, Seymour M., and Bogdonoff, Harriet E.: Blade Design Data for Axial-Flow Fans and Compressors. NACA ACR No. L5F07a, 1945.
4. Bogdonoff, Seymour M., and Hess, Eugene E.: Axial-Flow Fan and Compressor Blade Design Data at 52.5° Stagger and Further Verification of Cascade Data by Rotor Tests. NACA TN No. 1271, 1947.

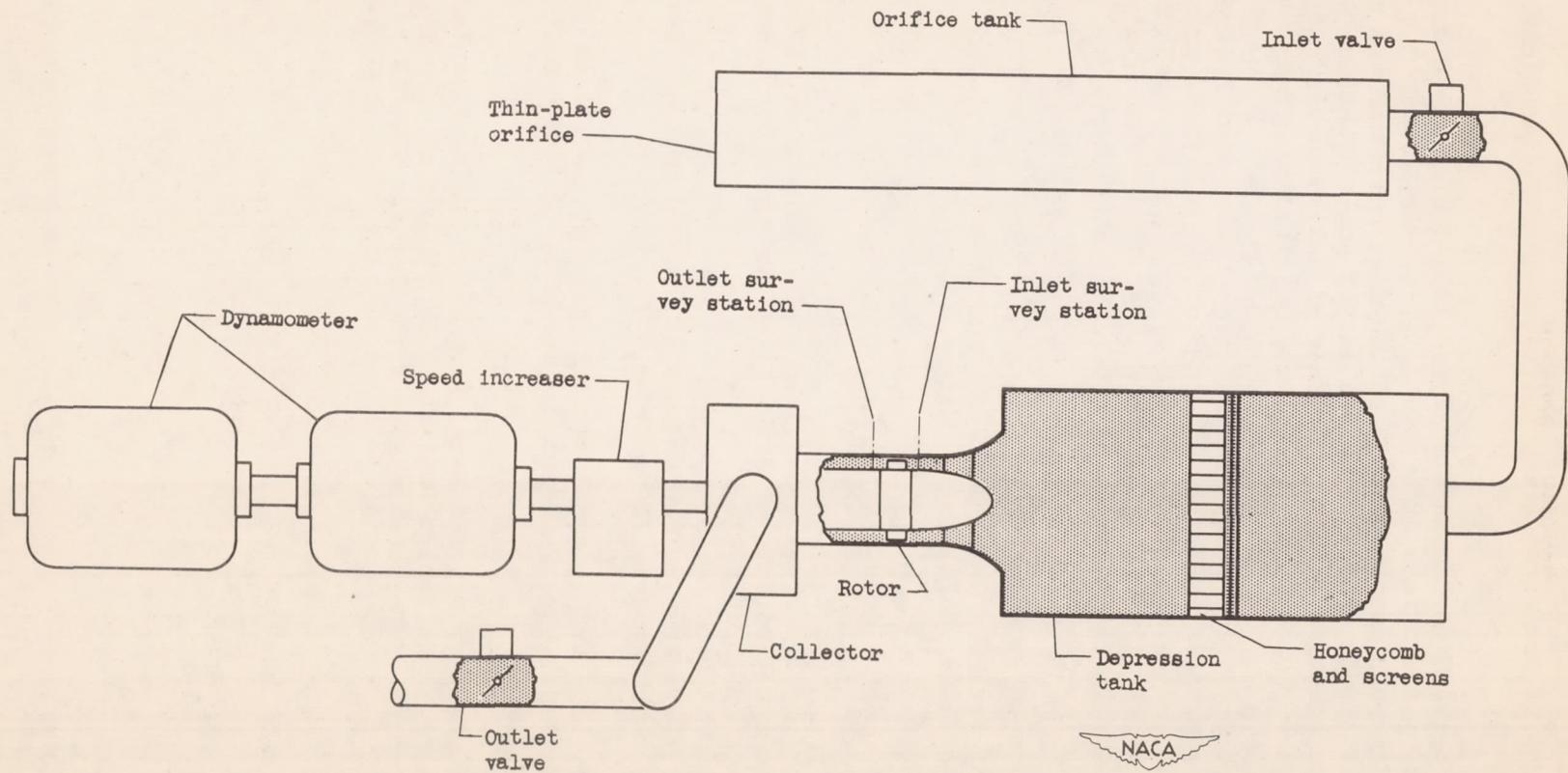
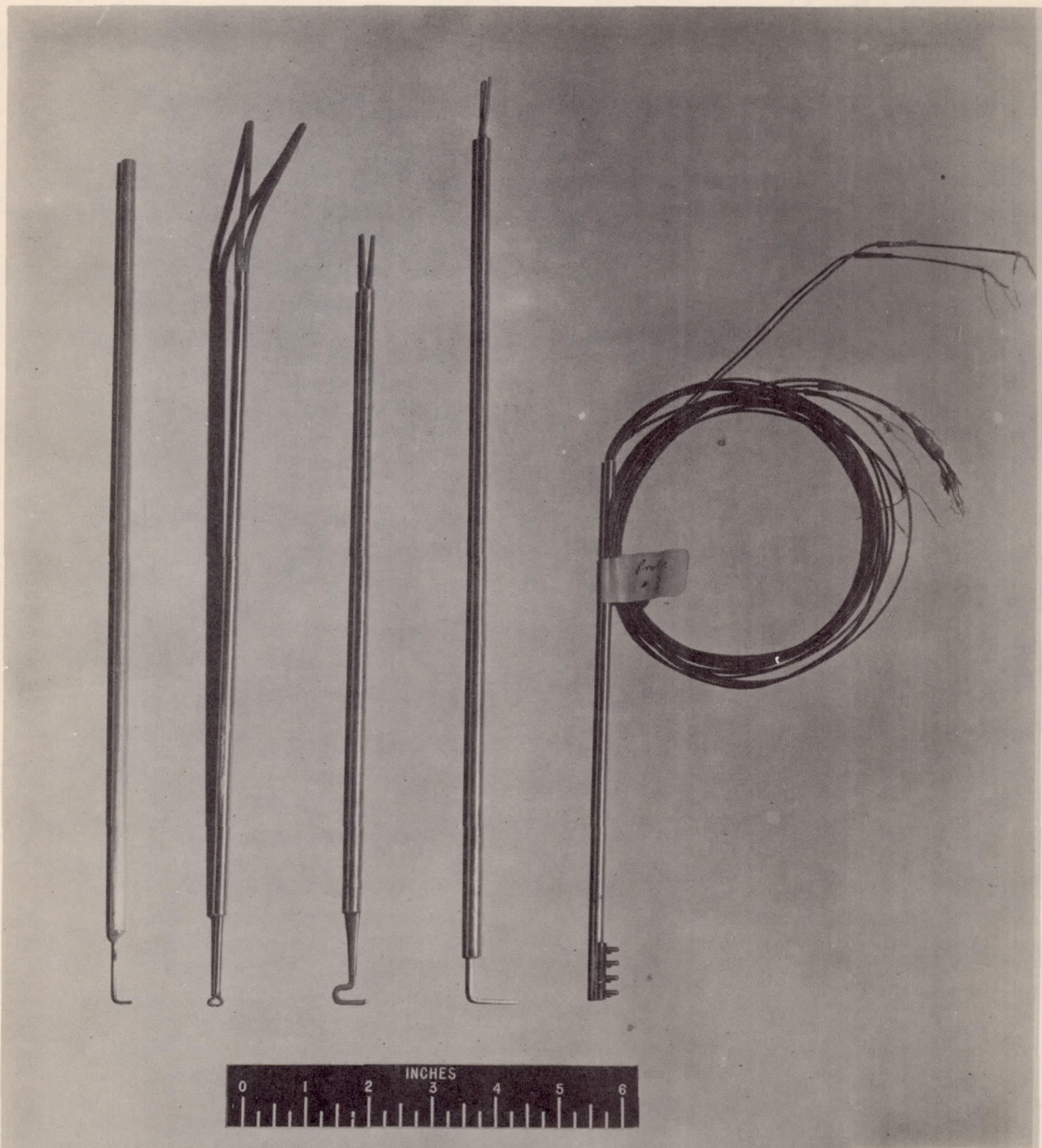


Figure 1. - Schematic diagram of compressor installation.



Total- pressure survey probe	Claw-type yaw tube	Static- pressure survey probe	Static- pressure survey probe	Thermo- couple rake
---------------------------------------	--------------------------	--	--	---------------------------

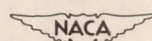

 C-20898
 3-16-48

Figure 2. - Instrumentation.

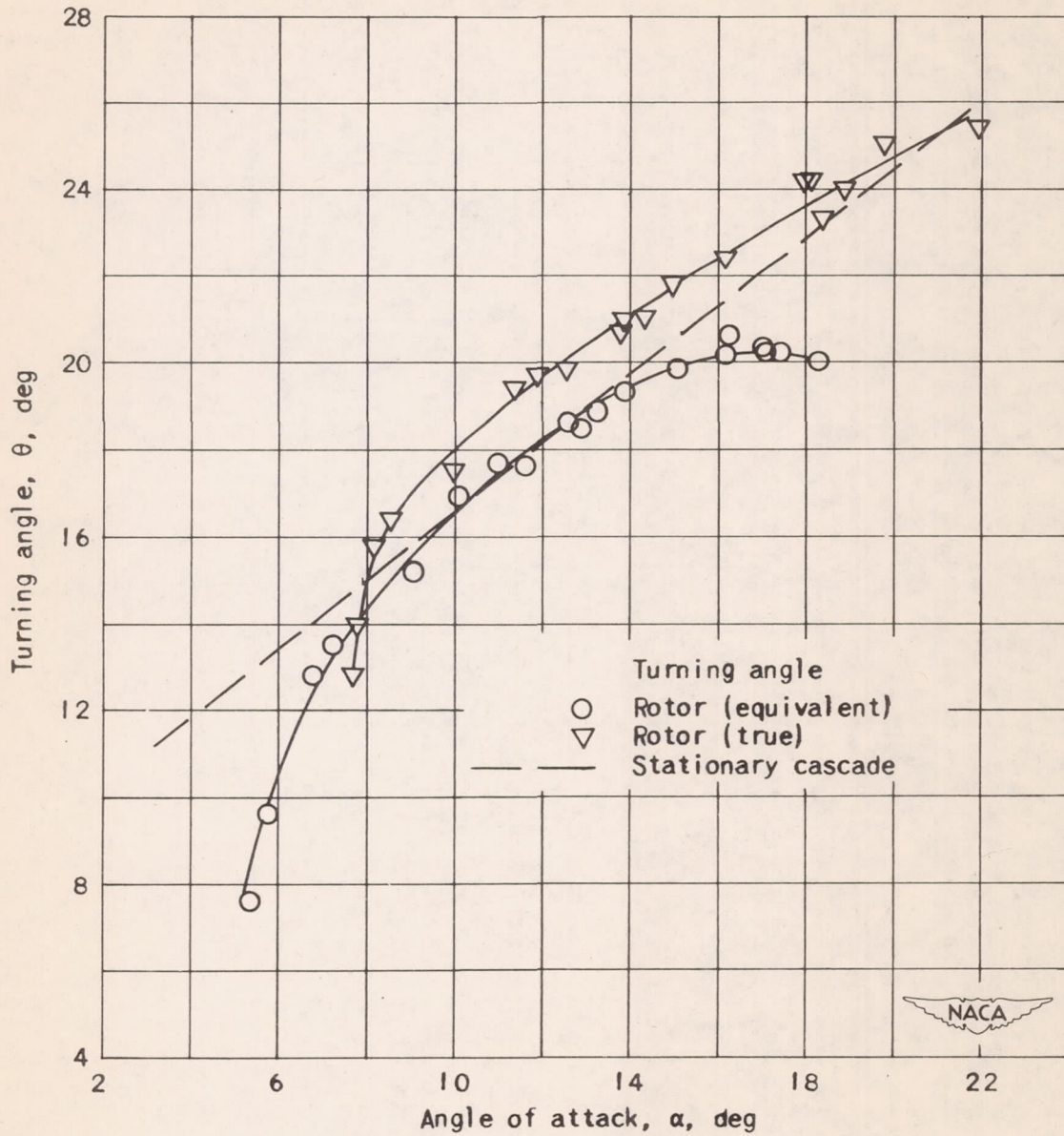


Figure 3. - Variation of turning angle at mean radius with angle of attack for design tip speed of 736 feet per second. Stationary cascade turning angles obtained by interpolation of data from references 3, 4, and unpublished data for solidity of 1.2 and camber of 9.6.

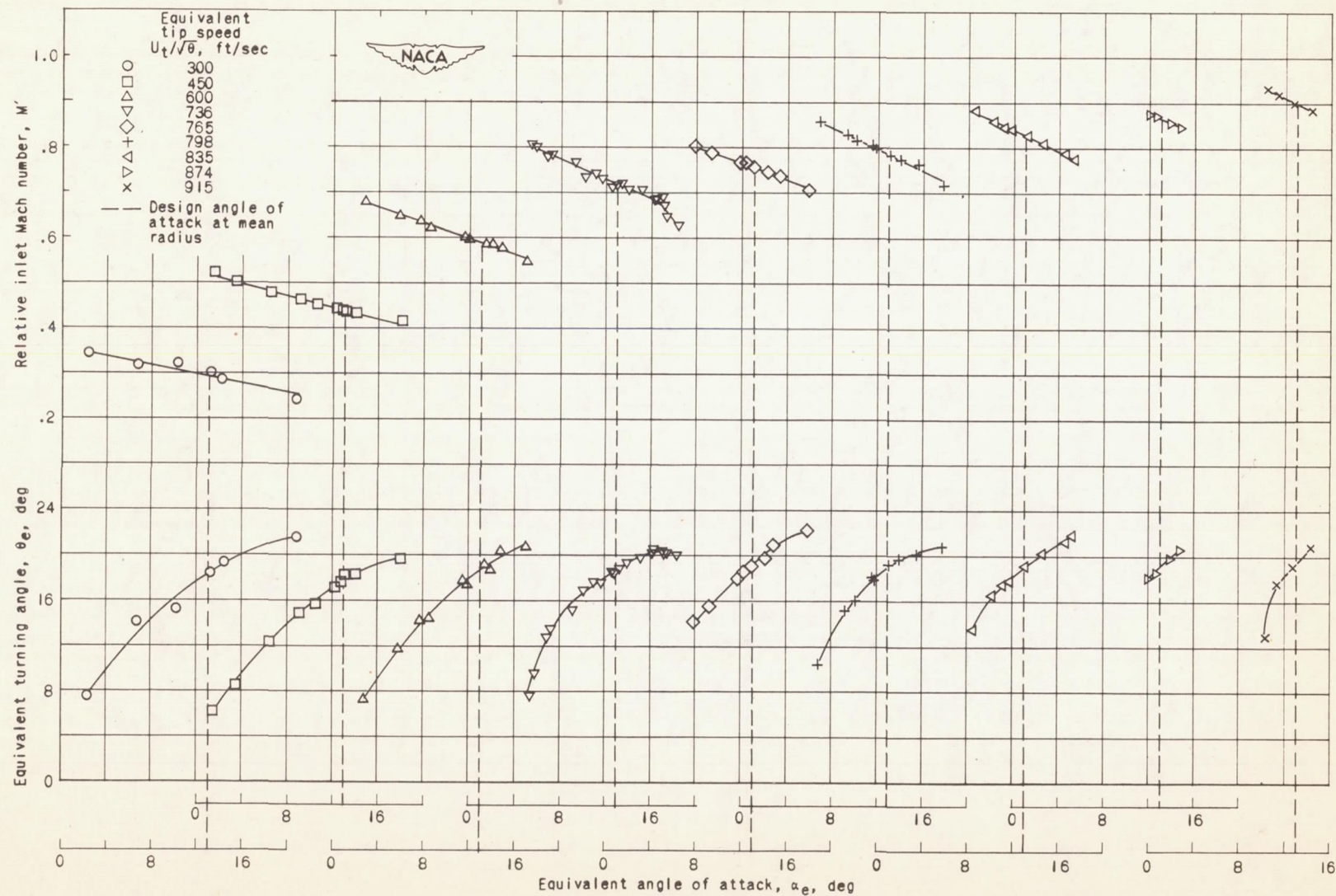


Figure 4. - Variation of equivalent turning angle and relative inlet Mach number with equivalent angle of attack for mean-radius conditions.

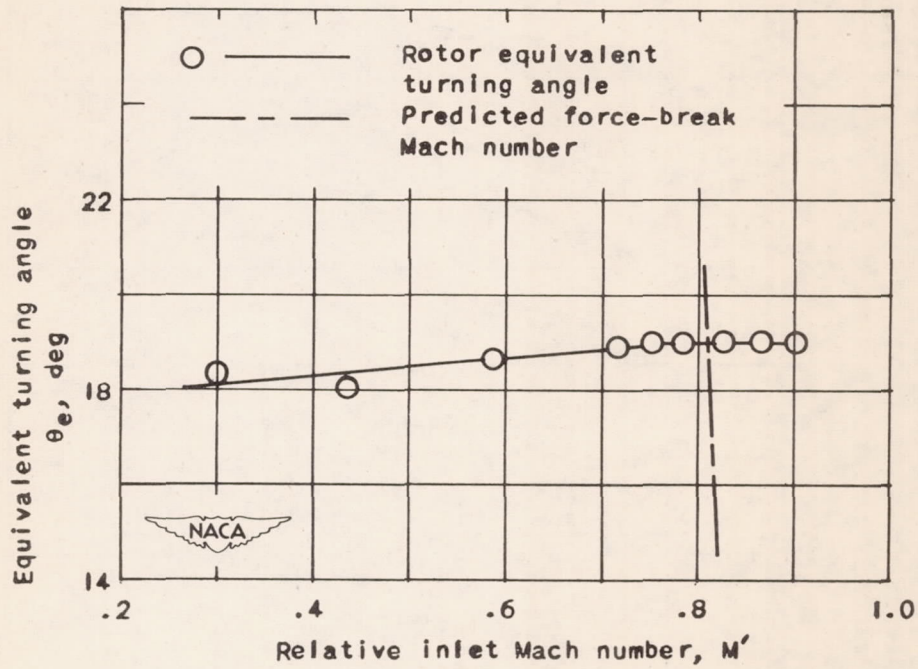


Figure 5. - Variation of equivalent turning angle with relative inlet Mach number for mean-radius conditions. Predicted force-break Mach number interpolated for angle of attack of 13° , stagger angle of 57.4° , and solidity of 1.2.

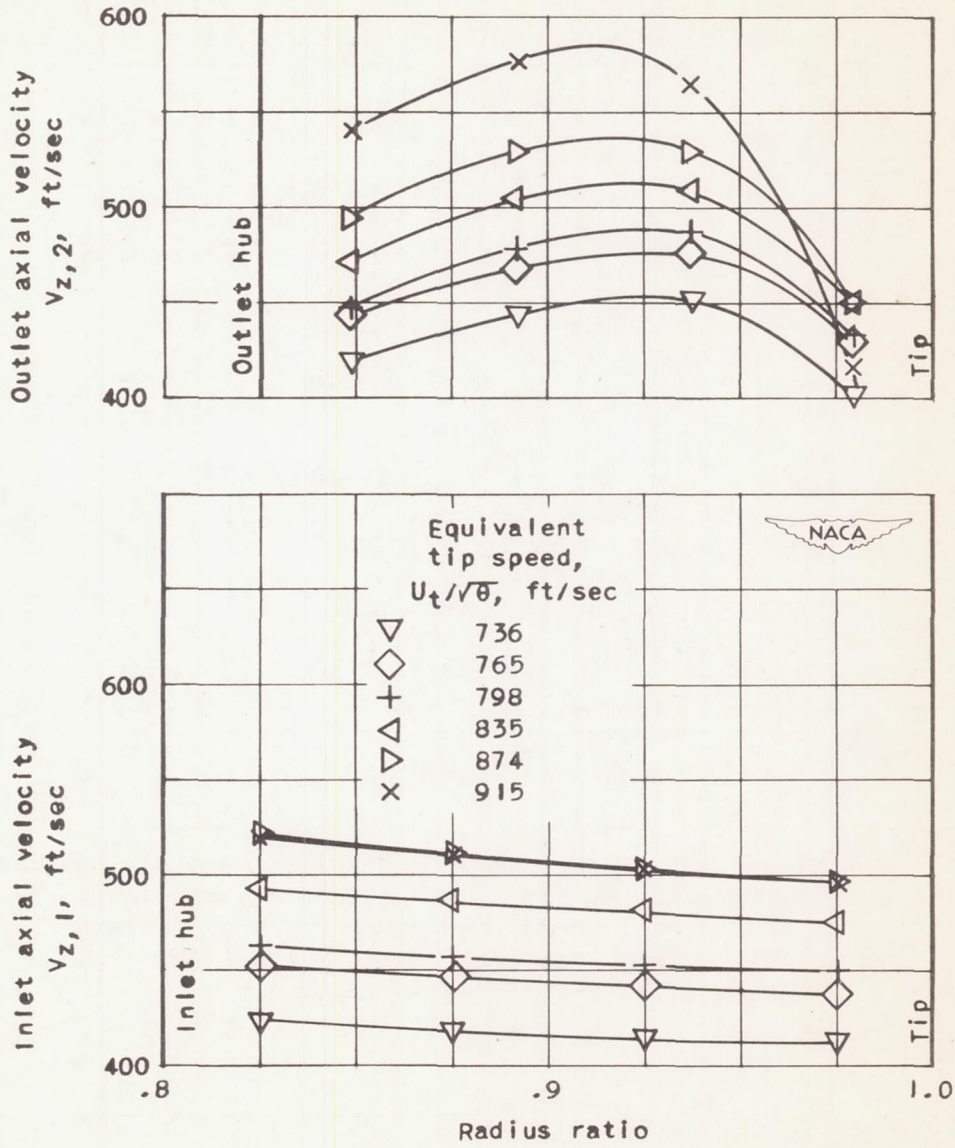


Figure 6. - Inlet and outlet axial velocity distribution for conditions near design flow.

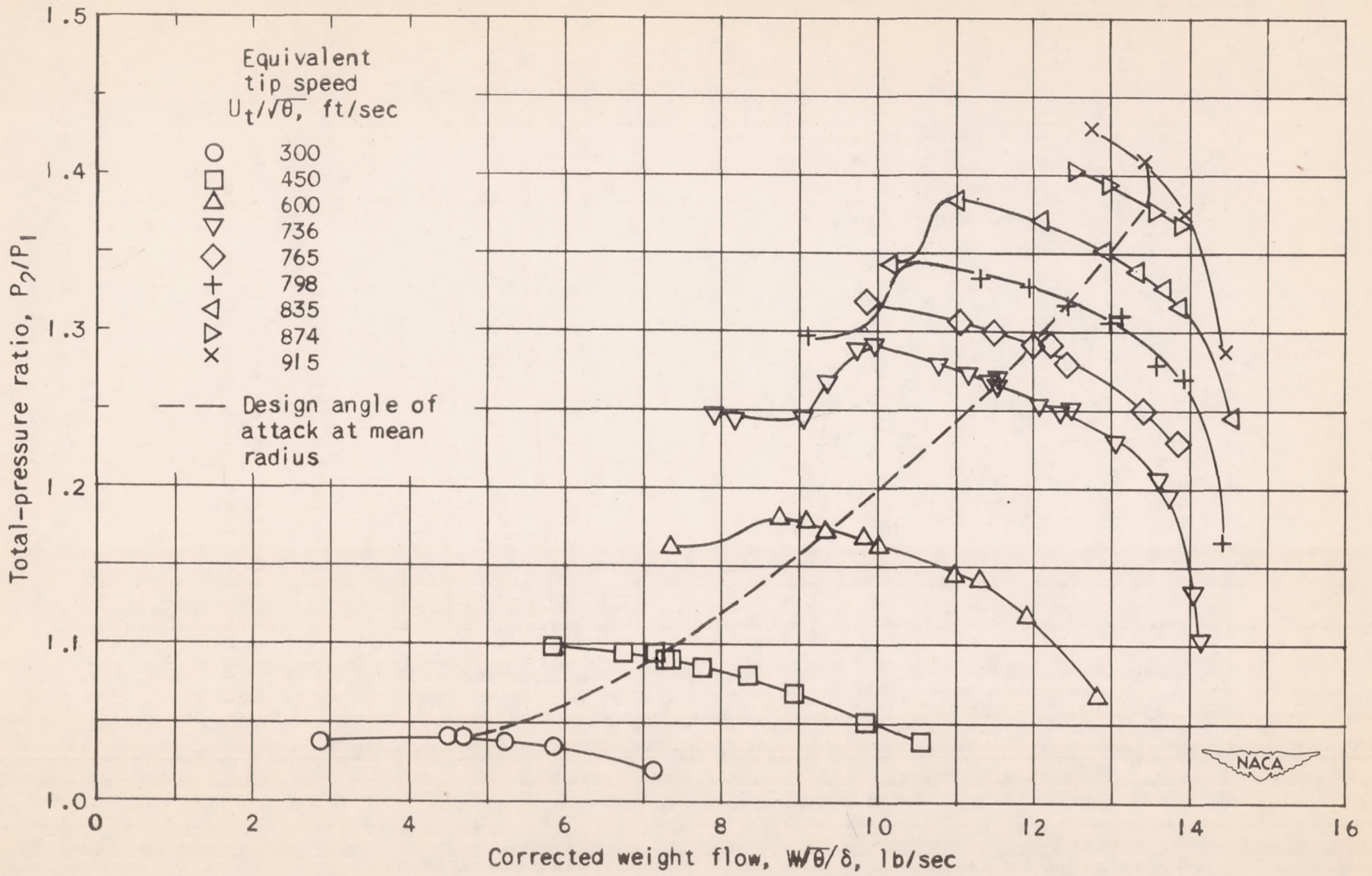


Figure 7. - Variation of total-pressure ratio with corrected weight flow.

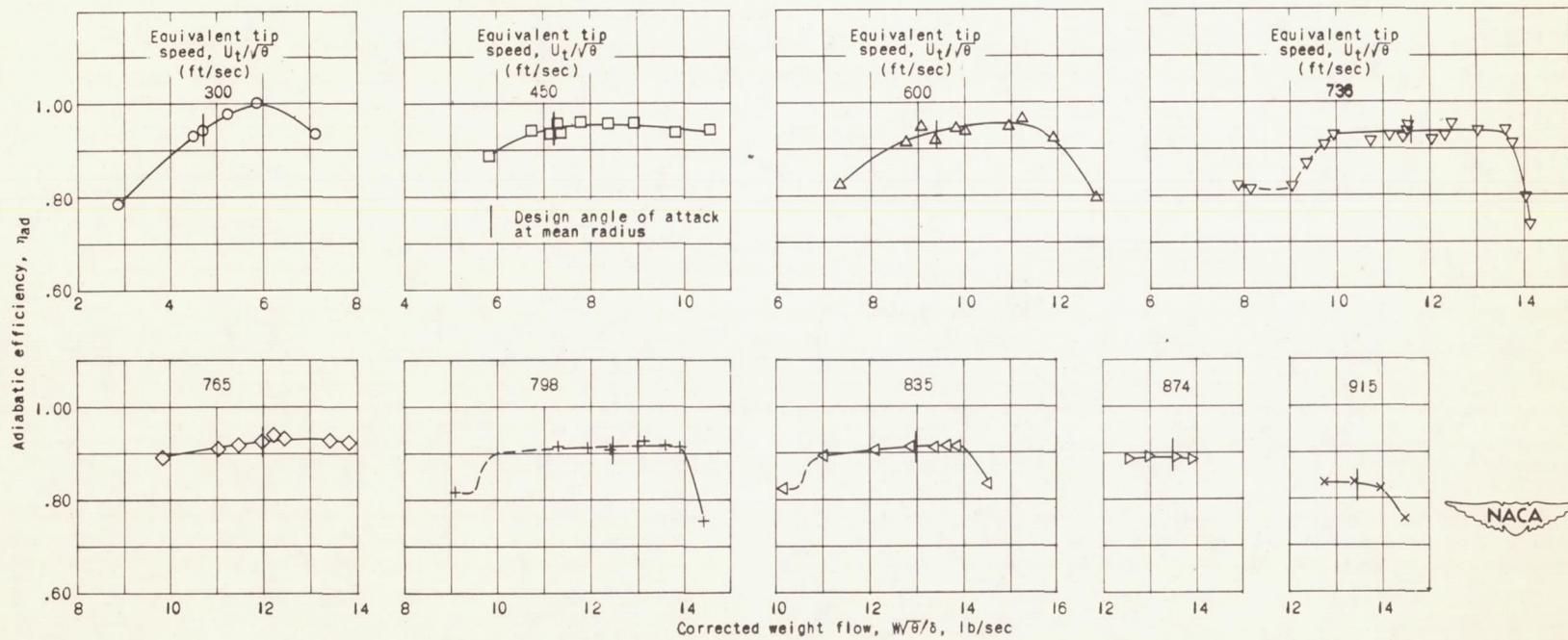
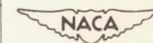


Figure 8. - Variation of adiabatic efficiency with corrected weight flow.



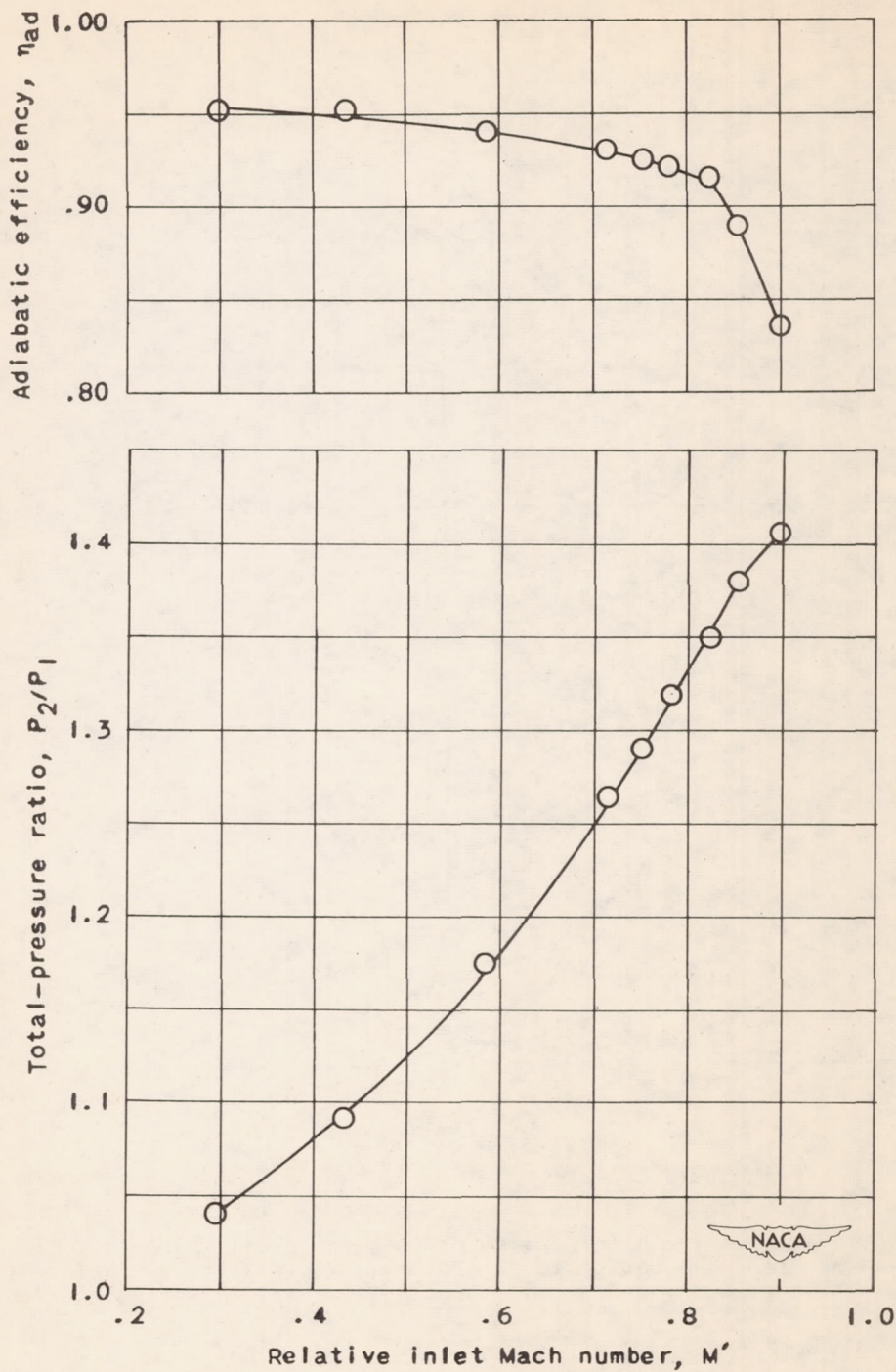
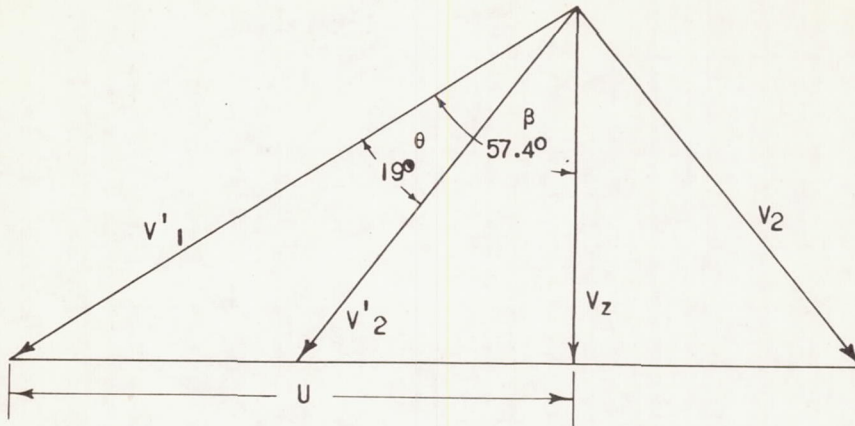
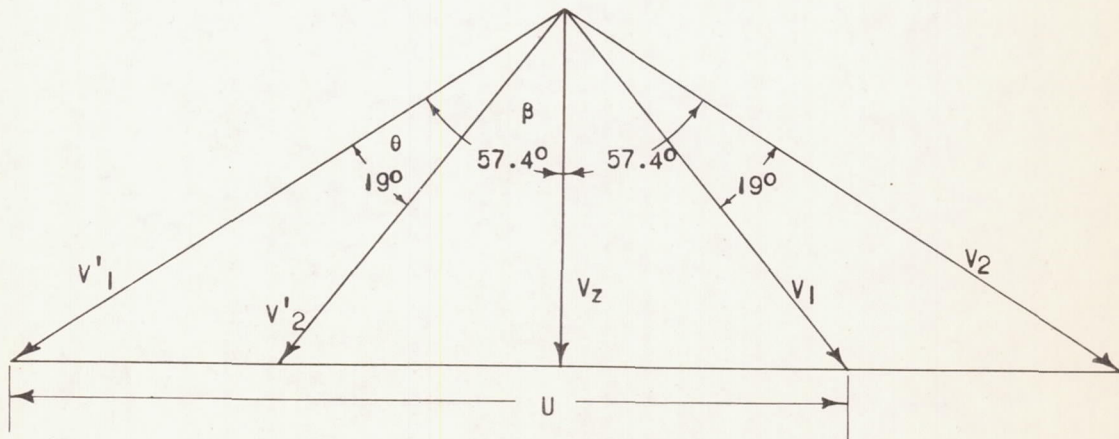


Figure 9. - Variation of adiabatic efficiency and total-pressure ratio with relative inlet Mach number.



(a) Diagram for rotor alone.



(b) Symmetrical diagram for complete stage.

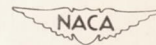


Figure 10. - Typical vector diagrams for constant axial velocity. Velocity of blade at any radius U ; absolute air velocity V ; relative air velocity V' ; stagger angle β ; turning angle θ ; subscripts: inlet measuring station 1; outlet measuring station 2; axial z .

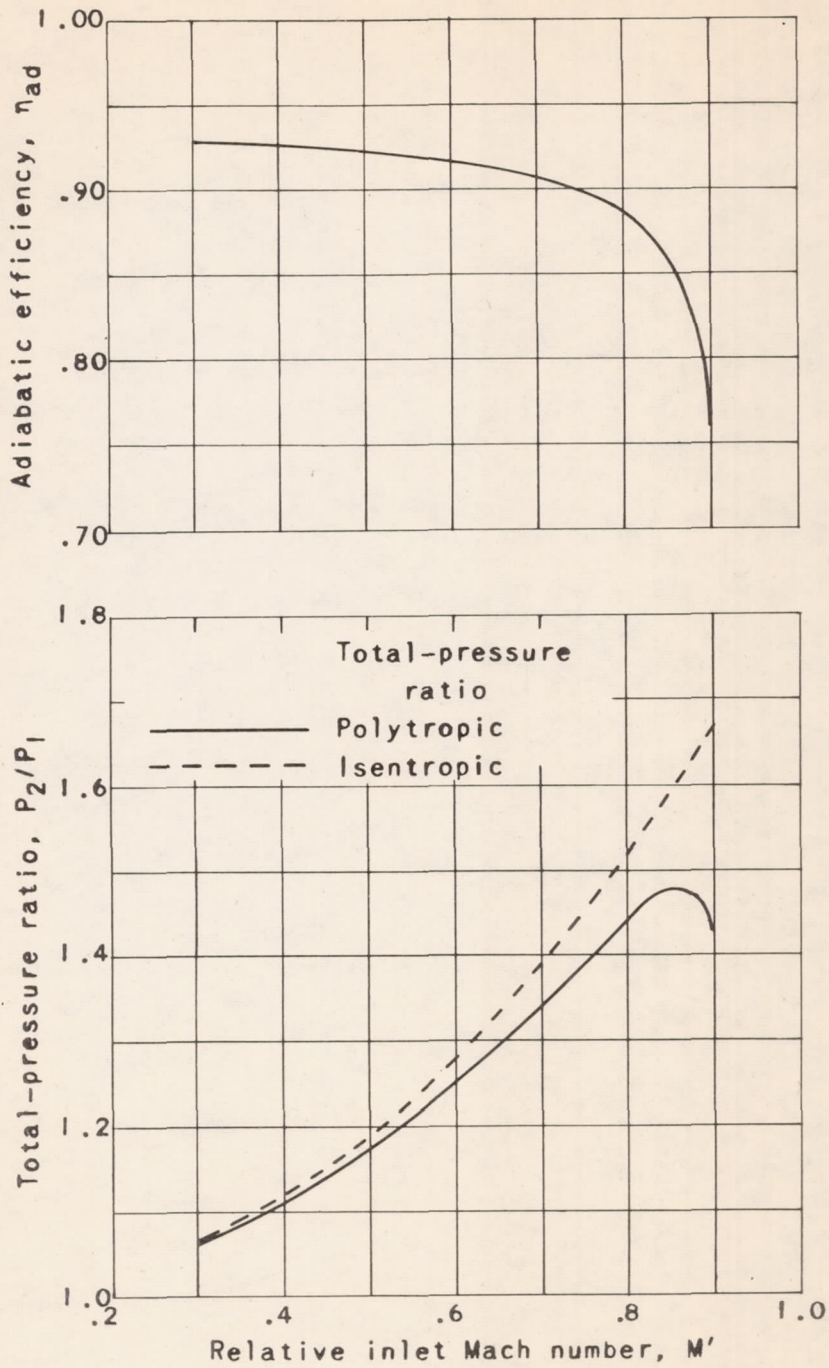


Figure 11. - Variation of theoretical performance values with relative inlet Mach number for complete stage based on symmetrical velocity diagram and stagger angle of 57.4° .